Received: 27 August 2019 | Revised: 6 January 2020 | Accepted: 9 January 2020

DOI: 10.1111/cas.14315

ORIGINAL ARTICLE

Cancer Science WILEY

Prediction of overall survival in resectable intrahepatic cholangiocarcinoma: IS_{ICC}-applied prediction model

Mengxin Tian[1] | Weiren Liu[1] | Chenyang Tao[1] | Zheng Tang[1] | Yufu Zhou[1] | Shushu Song[1] | Lei Jin[1] | Han Wang[1] | Xifei Jiang[1] | Peiyun Zhou[1] | Yuan Fang[1] | Weifeng Qu[1] | Zhenbin Ding[1] | Yuanfei Peng[1] | Xiutao Fu[1] | Shuangjian Qiu[1] | Jian Zhou[1,2] | Jia Fan[1,2] | Yinghong Shi[1]

[1]Key Laboratory of Carcinogenesis and Cancer Invasion of Ministry of Education, Department of Liver Surgery, Liver Cancer Institute, Zhongshan Hospital, Fudan University, Shanghai, China

[2]Institutes of Biomedical Sciences, Fudan University, Shanghai, China

Correspondence
Yinghong Shi, Department of Liver Surgery, Liver Cancer Institute, Zhongshan Hospital, Fudan University, 180 FengLin Road, Shanghai 200032, China.
Email: shi.yinghong@zs-hospital.sh.cn

Funding information
Shanghai Sailing Program, Grant/Award Number: 19YF1407800 and 19YF1404300; China Postdoctoral Science Foundation, Grant/Award Number: 2018M640343 and 2019T120305; National High Technology Research and Development Program (863 Program) of China, Grant/Award Number: 2015AA020401; Shanghai Committee of Science and Technology, China, Grant/Award Number: 16JC1404000; National Natural Science Foundation of China, Grant/Award Number: 81472674, 81530077, 81502486, 81773067, 81902963 and 81800790; Shanghai Municipal Education Commission; Shanghai Education Development Foundation; Shanghai Municipal Science and Technology Major Project

Abstract

Intrahepatic cholangiocarcinoma (ICC) remains a highly heterogeneous disease with poor prognosis. Tumor-infiltrating lymphocytes were predictive in various cancers, but their prognostic value in ICC is less clear. A total of 168 ICC patients who had received liver resection were enrolled and assigned to the derivation cohort. Sixteen immune markers in tumor and peritumor regions were examined by immunohistochemistry. A least absolute shrinkage and selection operator model was used to identify prognostic markers and to establish an immune signature for ICC (IS_{ICC}). An IS_{ICC}-applied prediction model was built and validated in another independent dataset. Five immune features, including $CD3_{peritumor\ (P)}$, $CD57_P$, $CD45RA_P$, $CD66b_{intratumoral\ (T)}$ and $PD\text{-}L1_P$, were identified and integrated into an individualized IS_{ICC} for each patient. Seven prognostic predictors, including total bilirubin, tumor numbers, CEA, CA19-9, GGT, HBsAg and IS_{ICC}, were integrated into the final model. The C-index of the IS_{ICC}-applied prediction model was 0.719 (95% CI, 0.660-0.777) in the derivation cohort and 0.667 (95% CI, 0.581-0.732) in the validation cohort. Compared with the conventional staging systems, the new model presented better homogeneity and a lower Akaike information criteria value in ICC. The IS_{ICC}-applied prediction model may provide a better prediction performance for the overall survival of patients with resectable ICC in clinical practice.

KEYWORDS
immune-infiltrating cells, intrahepatic cholangiocarcinoma, liver cancer, prognosis, survival prediction

1 | INTRODUCTION

Intrahepatic cholangiocarcinoma (ICC), arising from the epithelial cells of segmental or proximal branches of the bile duct, accounts for 5%-30% of all primary liver malignancies.[1] The incidence and mortality rates of ICC have increased globally over the past 30 years, indicating that ICC has become a growing clinical problem.[2,3] Surgical resection is the mainstay of curative treatment and is associated with improved survival in selected ICC patients.

Tian, Liu, Tao and Tang contributed equally to this work.

Tumor-infiltrating lymphocytes have been shown to be a determinant of carcinogenesis and progression, and may also serve as a predictor of patient response to neoadjuvant chemotherapy.[4,5] Wang et al[6] reported that IL-17A$^+$ immune cell infiltration was correlated with antitumor immune contexture and improved response to adjuvant chemotherapy in gastric cancer. In addition, Nywening et al[7] revealed that dual targeting of tumor-associated CCR2$^+$ macrophages and CXCR2$^+$ neutrophils could improve chemotherapeutic responses and enhance antitumor immunity by disrupting myeloid recruitment in pancreatic ductal adenocarcinoma. In colorectal cancer, CD8$^+$ and CD45RO$^+$ lymphocytes were found to be prognostic factors that might play a critical role in controlling tumor progression,[8] and were defined as a new component in the classification criteria of colorectal cancer.[9] Previously, we observed that intratumoral IL-17$^+$ and CD66b$^+$ immune cells were independent prognostic factors for long-term survival of ICC patients.[10] In addition, an elevated neutrophil/lymphocyte ratio (≥3) was able to predict worse survival for surgically resected ICC patients, including in patients that received neoadjuvant chemotherapy.[11] These results suggested that identification of robust prognostic factors may enhance the predictive power of the current staging systems for ICC patients. However, the nature of immune infiltration in ICC remains to be comprehensively explored.

In this study, we first investigated the immune microenvironment of ICC based on gene expression profiles from a public database. Then, we examined the histopathological expression levels of 16 immune markers in ICC tissue specimens. By using the least absolute shrinkage and selection operator (LASSO) Cox method on the basis of overall survival (OS), we developed an immune signature for ICC patients (IS_{ICC}) based on 5 prognostic immune features, and integrated the clinicopathological characteristics and IS_{ICC} into a new prognostic model. Finally, we compared the performance of this model with three existing staging systems.

2 | MATERIALS AND METHODS

2.1 | Patients

A retrospective study was carried out on a primary dataset of patients who received hepatic resection for ICC between February 2005 and July 2011 at the Department of Liver Surgery, Zhongshan Hospital. Standard liver resection techniques were applied.[12] Tumor stage was determined according to the American Joint Committee on Cancer (AJCC)/Union for International Cancer Control TNM classification system. Tumor differentiation was graded according to the Edmonson-Steiner criteria.[13] Patients were confirmed to have ICC with histopathological evidence before study enrollment, with no history of other cancers, with Child-Pugh class A, and with no history of anticancer therapy before surgery; all these patients underwent complete resection of tumors, and showed no signs of distant or intrahepatic metastasis. A total of 280 patients were enrolled. Data were censored at the last follow up for patients without recurrence or death. OS and recurrence-free survival (RFS) was defined as the interval between the date of surgery to the date of death or recurrence. The study was approved by the institutional review board of Zhongshan Hospital and was conducted in accordance with the standards of the Declaration of Helsinki. Informed consent was obtained from each patient prior to treatment.

Patients were randomly assigned to the derivation cohort (n = 168) or the validation cohort (n = 112) (Figure S1). As summarized in Table 1, no significant differences were observed in the clinicopathological characteristics of ICC between the two cohorts. HBsAg-positive patients accounted for 39.9% of individuals in the derivation cohort and 45.5% in the validation cohort, respectively. The median levels of AFP, CEA and CA19-9 were 2.7 ng/mL, 2.5 μg/mL and 37.7 U/mL in the derivation cohort, respectively. During the follow-up period, 71.4% of all patients (200/280) developed recurrence and 62.5% (175/280) died. For the entire cohort, the median follow-up time was 44.5 months (range, 7.3-109.5 months), the median OS was 28.3 months (95% CI, 20.8-35.8 months), and the 1, 3 and 5-year OS rates were 73.4%, 44.4% and 32.4%, respectively.

2.2 | Tissue microarray construction and immunohistochemistry

Tissue microarray (TMA) construction was performed as previously described.[14,15] Briefly, two representative areas with infiltrating lymphocytes were selected on H&E-stained slides. Duplicate cores (2 μm in diameter) were taken, arrayed and re–embedded from tumor and peritumor regions. Fourteen monoclonal and two polyclonal antibodies against CD3, CD4, CD8, CD14, CD20, CD27, CD45RO, CD45RA, CD57, CD66b, CD68, CD103, Foxp3, CXCR5, PD-L1 and PD1 were used for staining, as reported previously.[15] To evaluate peritumoral and intratumoral infiltrating immune cells, the three most representative and independent fields were selected and photographed at ×200 magnification. Identical settings were used for each photograph. The numbers of positive cells were counted and recorded using a computer-automated method (Image-Pro Plus 6.0, Media Cybernetics) as previously described.[15,16] Figure S2 presents the spot and the captured spot (×200) with image software. The mean value of positive cells was used for statistical analysis. More detailed information is presented in the Supplementary Methods and Table S1.

2.3 | Establishment of an immune signature for intrahepatic cholangiocarcinoma (IS_{ICC}) patients

The least absolute shrinkage and selection operator (LASSO) method, which is suitable for the analysis of high-dimensional data, was used to select the most predictive immune features from the derivation cohort on the basis of OS and then construct a multi-immune feature

TABLE 1 Demographic, clinical and tumor characteristics of patients with intrahepatic cholangiocarcinoma

Patient demographics	Derivation cohort (n = 168)	Validation cohort (n = 112)	*P*-value
Age, year			
<60 years	86 (51.2%)	67 (59.8%)	.19
≥60 years	82 (48.8%)	45 (40.2%)	
Sex (male), n (%)	99 (58.9%)	74 (66.1%)	.28
Etiology			
HBV	67 (39.9%)	51 (45.5%)	.57
HCV	3 (2.8%)	1 (0.9%)	
Others	98 (58.3%)	60 (53.6%)	
AFP, ng/mL	2.7 (1.9, 4.8)	2.7 (2.0, 4.7)	.51
CEA, μg/mL	2.5 (1.4, 4.1)	2.2 (1.4, 4.5)	.67
CA19-9, U/mL	37.7 (16.0, 283.2)	37.3 (15.7, 178.6)	.63
Albumin, g/L	43.0 (40.0, 45.0)	43.0 (40.0, 46.0)	.55
Bilirubin, μmol/L	11.8 (8.8, 15.3)	11.8 (9.3, 16.3)	.62
ALT, IU/L	20.5 (13.8, 35.3)	21.0 (15.0, 36.5)	.60
GGT, U/L	48.0 (31.0, 100.3)	46.55 (31.8, 92.0)	.51
Platelets, 10^3/μL	176.5 (133.8, 217.3)	190.5 (152.0, 216.3)	.20
Tumor nodularities, n (%)			
1	134 (79.8%)	96 (85.7%)	.44
2	20 (11.9%)	9 (8.0%)	
≥3	14 (8.3%)	7 (6.3%)	
Tumor diameter, cm	6.0 (4.4, 8.0)	6.0 (4.4, 9.0)	.96
Tumor differentiation, n (%)			
I-II	117 (69.6%)	74 (66.1%)	.62
III-IV	51 (30.4%)	38 (33.9%)	
Vascular invasion (yes), n (%)	7 (4.2%)	7 (6.3%)	.61
Lymphoid metastasis (yes), n (%)	9 (5.4%)	8 (7.1%)	.72
Direct invasion and local extrahepatic metastasis (yes), n (%)	2 (1.2%)	0 (0%)	.52
Occlusion, min			
<15 min	114 (67.9%)	67 (59.8%)	.21
≥15 min	54 (32.1%)	45 (40.2%)	

Note: Values are presented as patient number (%) or median (Q1, Q3).

Abbreviations: AFP, α-fetoprotein; ALT, alanine aminotransferase; CA19-9, carbohydrate 19-9; CEA, carcino-embryonic antigen; GGT, γ-glutamyl transpeptidase; HBV, hepatitis B virus; HCV, hepatitis C virus; VI, vascular invasion.

model.[17] The "glment" package was used to perform LASSO Cox regression analysis.

2.4 | Construction of IS_{ICC}-applied prediction model

For the model to achieve satisfactory performance, all the variables with $P < .1$ in the univariate analysis were identified through a backward stepwise selection process based on the Akaike information criterion (AIC).[18] The final prognostic model was determined on the basis of the lowest AIC instead of the variables ($P < .05$) selected in the multivariate analysis. The IS_{ICC}-applied prediction model was calculated for each patient based on IS_{ICC} and clinical parameters.

2.5 | Statistical analysis

Statistical analyses were conducted with R version 3.1.0 (R Foundation, Vienna, Austria). Demographic and clinicopathological characteristics were presented as percentages or median values. Categorical variables were analyzed using Pearson's χ^2 test or Fisher's exact test. The Wilcoxon test or Student's *t* test was used

to evaluate continuous variables. OS curves were plotted using the Kaplan-Meier method and compared using the log-rank test. The performance of three staging systems and the IS_{ICC}-applied prediction model were compared with the rcorrp.cens package in Hmisc[19] and validated in the validation cohort. According to the highest χ^2-value defined by Kaplan-Meier survival analysis and log-rank tests, ICC patients were categorized into three subgroups with X-tile software version 3.6.1 (Yale University School of Medicine, New Haven, CT, USA).[20] To investigate the performance of stratified IPM and three traditional staging systems, we chose the corrected AIC (AICc)[21] to evaluate the correlation of the staging systems with patient survival and Wald χ^2 tests to determine homogeneity.[22] A *P*-value < .05 was considered statistically significant.

3 | RESULTS

3.1 | Characterization of the immune microenvironment of ntrahepatic cholangiocarcinoma

To investigate the characteristics of immune microenvironment, a public dataset (GSE76297) of 91 ICC patients was obtained from the Gene Expression Omnibus of our study.[23] By using the CIBERSORT-inferred relative fractions of different immune cell types, we observed depletion of intratumoral plasma cells, $CD8^+$ T cells, nature killer (NK) cells and monocytes, along with significant enrichment of T follicular helper (Tfh) cells, macrophage cells and dendritic cells (Figure 1A). Evaluation of the infiltrating immune cells using immunohistochemistry revealed similar results, with a decrease of $CD4^+$, $CD8^+$, $CD20^+$ and $CD27^+$ lymphocytes and an increase of $Foxp3^+$, $CXCT5^+$ and $CD103^+$ lymphocytes. These results suggested an immune-suppressive intratumoral immune microenvironment with loss of effector immune cells and accumulation of suppressive immune cells.

Correlation analysis was conducted to investigate the correlations of immune cells in the GSE76297 dataset. Three clusters were identified in ICC tissues, characterized by markers of exhausted immune response (neutrophils and eosinophils), adaptive T response (plasma and NK cells) or both (CD8, Tregs and monocytes) (Figure 1B left). To confirm these results, the density of 16 immune infiltrations was examined using ICC TMA (Figure S3). Figure 1B (right), which revealed three dominant clusters characterized by adaptive T response (CXCR5, CD20 and CD45RA; CD3, CD4, CD8, CD27 and CD45RO) or exhausted immune response (CD20, CD27 and CD45RA).

In the T cell network, the local coordination underlines the existence of tumor-microenvironment compartments with different compositions that might influence the mobility and activity of T and B cells along with tumor progression.[24] We constructed immune networks to evaluate the interactions of immune components in GSE76207 and 280 samples of ICC tissues. Figure 1C (left) reveals 2 independent networks with similar subnetworks of T cells (CD4, CD8, NK and Tregs). Interestingly, it was observed that CD4 might work as an important hub connecting adaptive T responses (NK, CD8 and Tregs) and exhausting immune response (plasma cells, monocytes or neutrophils) within peritumoral and intratumoral tissues. The network of immune features in 280 ICC tissue samples presented a similar pattern of separation between tumor and peritumor regions, while it was revealed that $CD103^+$ cells may function as a connection between the two immune networks (Figure 1C right). We observed a similar coordination of $CD4^+$ cells in histological evidence-based immune populations, which was consistent with the results of GSE76297.

3.2 | Establishment of IS_{ICC}

Using the LASSO Cox method, 5 out of 32 prognostic immune features were identified as having the highest predictive values on the basis of OS, including $CD3_{peritumor\ (p)}$, $CD57_P$, $CD45RA_P$, $CD66b_{intratumor\ (T)}$ and $PD\text{-}L1_P$ (Figure 1D). The expression pattern of 5 selected immune features is presented in Figure 1E. We applied a novel equation to each patient based on their levels of these specific factors (Figure 1F): the IS_{ICC} = (the level of $CD45RA_P \times 10.602$ − the level of $CD3_P \times 6.025$ − the level of $CD57_P \times 31.013$ + the level of $CD66b_T \times 5.421$ − the level of $PD\text{-}L1_P \times 3.252) \times 10^{-4}$. In this formula, the expression levels of the corresponding immune features refer to the numbers of positively stained cells in tumor or non–tumor tissues in the histological analysis.

3.3 | Selection of prognostic factors

Eleven variables with *P* < .1 were identified through univariate analysis (Table 2). Backward stepwise selection was performed using the lowest AIC and Cox proportional hazards regression modeling. Seven predictors were associated with the OS of patients with operable ICC, in which total bilirubin (95% CI, 1.000-1.014, *P* = .046), tumor numbers (95% CI, 1.205-4.289, *P* = .01) and IS_{ICC} (95% CI, 7.734-131.243, *P* < .001) were independent prognostic factors for OS of ICC patients, while CEA (95% CI, 1.998-2.496, *P* = .05), CA19-9 (95% CI, 0.981-2.184, *P* = .06), GGT (95% CI, 0.901-2.194, *P* = .13) and HBsAg (95% CI, 0.477-1.082, *P* = .11) also tended to be associated with prognosis. Figure 2A indicates that the C-index values of IS_{ICC} scores (derivation cohort, 0.673; validation cohort, 0.651) were better than those of selected prognostic predictors in both cohorts (derivation cohort, 0.513-0.612; validation cohort, 0.498-0.625).

3.4 | Construction and performance of IS_{ICC}-applied prediction model

The 7 prognostic factors were integrated into an IS_{ICC}-applied prediction model, the formula of which was = 79.615 − 4.779 × the status of HBsAg + 0.101 × total bilirubin + 4.926 × the status of GGT + 5.504 × the status of CA19-9 + 6.593 × the status of CEA + 10.946 × the status of lymphoid metastasis − 0.057 × the status of tumor numbers + 50 × IS_{ICC}. Different values were assigned for

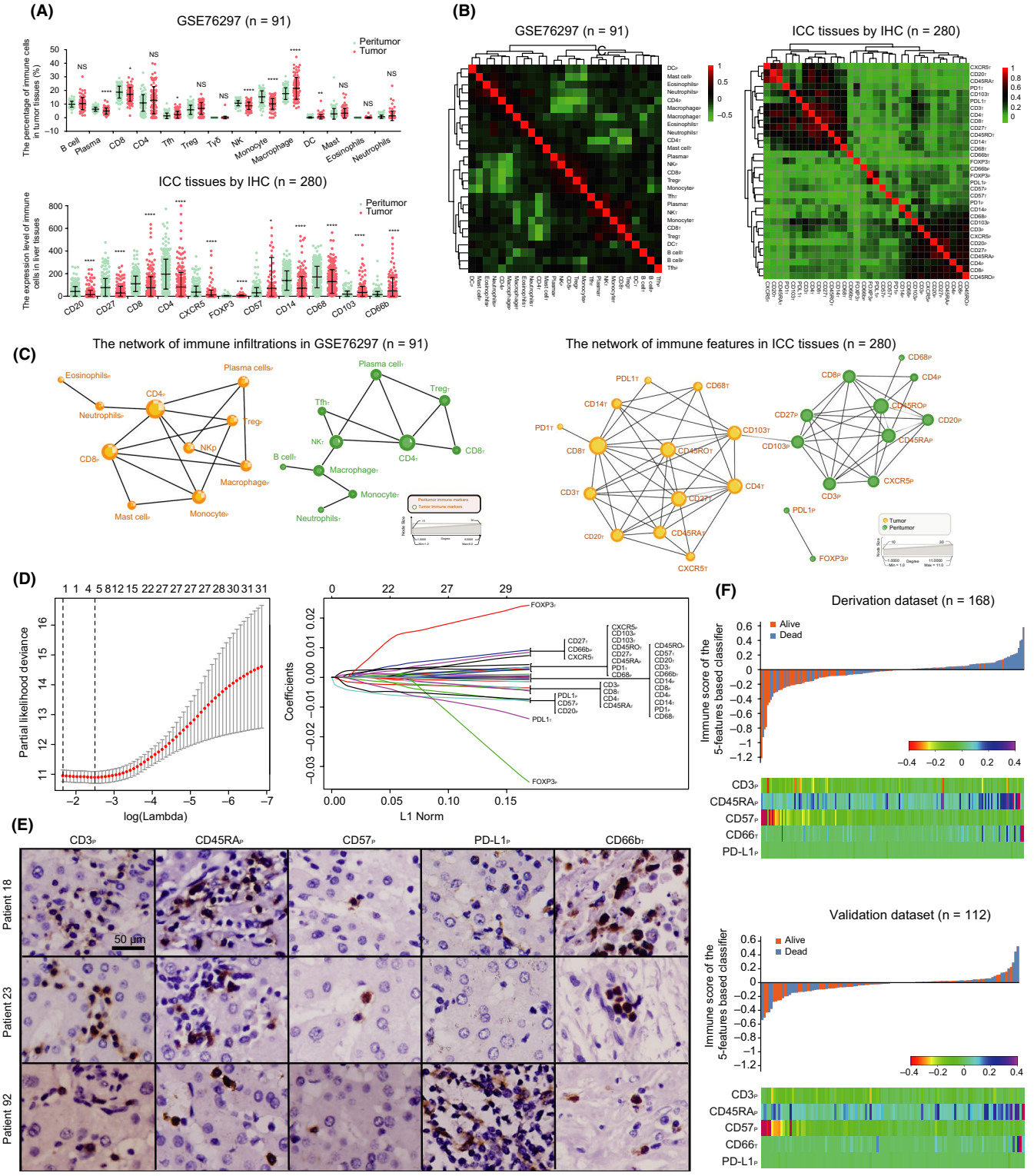

FIGURE 1 Characterization of immune microenvironment and selection of immune features by using least absolute shrinkage and selection operator (LASSO) Cox analysis in intrahepatic cholangiocarcinoma (ICC) patients. A, Comparison of immune cells between tumor and adjacent non–tumor tissues in the GSE76297 dataset (upper panel) and 280 ICC specimens (lower panel). B, Correlation matrix followed by unsupervised hierarchical clustering in GSE76297 dataset (left) and 280 ICC specimens (right). C, The immune network of immune infiltrations in GSE76297 (left) and 280 ICC specimens (right). D, Five immune features selected using LASSO Cox regression analysis. Left panel: The two dotted vertical lines were drawn at the optimal scores by minimum criteria and 1-s.e. criteria. Right panel: LASSO coefficient profiles of the 32 features. E, Expressions of selected prognostic features in ICC, including $CD3_P$, $CD45RA_P$, $CD57_P$, $PD\text{-}L1_P$ and $CD66b_T$ in 3 different patients. Bar, 20 μm. F, IS_{ICC} distribution of the 5 prognostic features in the derivation dataset and the validation dataset. Upper panel: IS_{ICC} distribution and patient survival status. Lower panel: heatmap presenting density of the 5 features in ICC patients

TABLE 2 Cox proportional hazards regression analysis of the association between variables and overall survival

	Univariate analysis			Multiple analysis		
Variable	**HR**	**95%CI**	***P*-value**	**HR**	**95%CI**	***P*-value**
HBsAg (yes/no)	0.631	0.427-0.933	.02	0.718	0.477-1.082	.11
CEA (≥5/<5, ng/mL)	2.029	1.305-3.152	.002	1.578	1.998-2.496	.05
CA19-9 (≥37/<37, U/mL)	1.466	1.003-2.142	.048	1.464	0.981-2.184	.06
TB, μmol/L	1.008	1.001-1.015	.03	1.007	1.000-1.014	.046
GGT (≥40/<40, U/L)	1.813	1.194-2.754	.005	1.406	0.901-2.194	.13
Tumor numbers						
1 nodule						
2 nodules	1.153	0.641-1.263	.63	0.996	0.543-1.826	.99
≥3 nodules	2.275	0.641-1.263	.006	2.273	1.205-4.289	.01
IS_{ICC}	20.949	5.947-73.796	<.001	31.859	7.734-131.243	<.001
Tumor diameter, cm	1.067	1.015-1.122	.01			
Tumor differentiation (I-II/III-IV)	1.495	1.010-2.213	.045			
Lymphoid metastasis (yes/no)	2.14	0.988-4.636	.05			
Blood loss volume, mL	1.001	1.000-1.001	.006			

Abbreviations: CA19-9, carbohydrate antigen 19-9; CEA, carcino-embryonic antigen; GGT, γ-glutamyl transpeptidase; HBsAg, hepatitis B surface antigen; IS_{ICC}, immune signature for ICC; TB, total bilirubin.

calculation according to the status of these parameters: for HBsAg, a positive status was defined as 2, while a negative status was defined as 1; for the status of GGT, a GGT level <40 U/L was defined as 0 and ≥40 U/L as 1; CEA level <5 μg/mL was defined as 0, CEA level ≥5 μg/mL was equivalent to 1; CA19-9 level <37 μg/mL was defined as 0, while CA19-9 ≥37 μg/mL was equivalent to 1; a positive lymphoid metastasis status was defined as 1 and negative as 0; and for tumor numbers, the presence of one tumor was defined as 1, two as 2 and >2 as 3.

Compared to three traditional staging systems for ICC, the IS_{ICC}-applied prediction model provided better predictive efficacy for resectable ICC (Figure 2B). In the derivation cohort, the C-index of the IS_{ICC}-applied prediction model was 0.719 (95% CI, 0.660-0.777), which was higher than the C-index values of AJCC 7th, Nathan and LCSGJ, which were 0.553 (95% CI, 0.506-0.600), 0.552 (95%CI, 0.505-0.559), and 0.558 (95% CI, 0.509-0.606), respectively. Similarly, the C-index of the IS_{ICC}-applied prediction model (0.667 [95% CI, 0.581-0.732]) in the validation cohort was also higher than the C-index values of the three traditional staging systems: AJCC 7th, 0.578 (95% CI, 0.522-0.636); Nathan, 0.570 (95% CI, 0.514-0.626); and LCSGJ, 0.577 (95% CI, 0.519-0.635).

3.5 | Stratifying risk of IS_{ICC}-applied prediction model in intrahepatic cholangiocarcinoma

The optimal cutoff scores of the IS_{ICC}-applied prediction model were determined using the X-tile software,[20] and the derivation cohort and the validation cohort were each categorized into three subgroups (score 1:0 to 78.3; score 2:78.3 to 87.7; score 3: more than 87.7) (Figure S4). Kaplan-Meier analysis indicated that both cohorts were well stratified (the derivation cohort: score 1 vs 2: $P < .001$; score 2 vs 3: $P < .001$; the validation cohort: score 1 vs 2: $P = .008$; score 2 vs 3: $P = .04$).

Furthermore, in this study, we used the corrected AIC values and homogeneity analysis to assess the prognostic efficacy of traditional staging systems and the IS_{ICC}-applied prediction model. In the derivation cohort, the stratification of the IS_{ICC}-applied prediction model showed the highest homogeneity (39.3) and the lowest AIC value (1017.5) (Table 3). A similar trend was observed in the validation cohort.

4 | DISCUSSION

Immune cell infiltration is a common feature in various types of cancer,[25] but the roles of lymphocytes in tumor progression and individualized survival prediction remain to be explored in ICC patients. In this study, we constructed an individualized immune signature and developed a novel immune prognostic score for ICC patients. The histological evidence-based immune features enhanced the performance of survival prediction, suggesting that the novel clinical and IS_{ICC}-applied prediction model may be superior to the three existing staging systems for selected ICC (Figure 3).

To investigate the characteristics of the immune microenvironment, we analyzed the gene expression profiles from GEO to assess

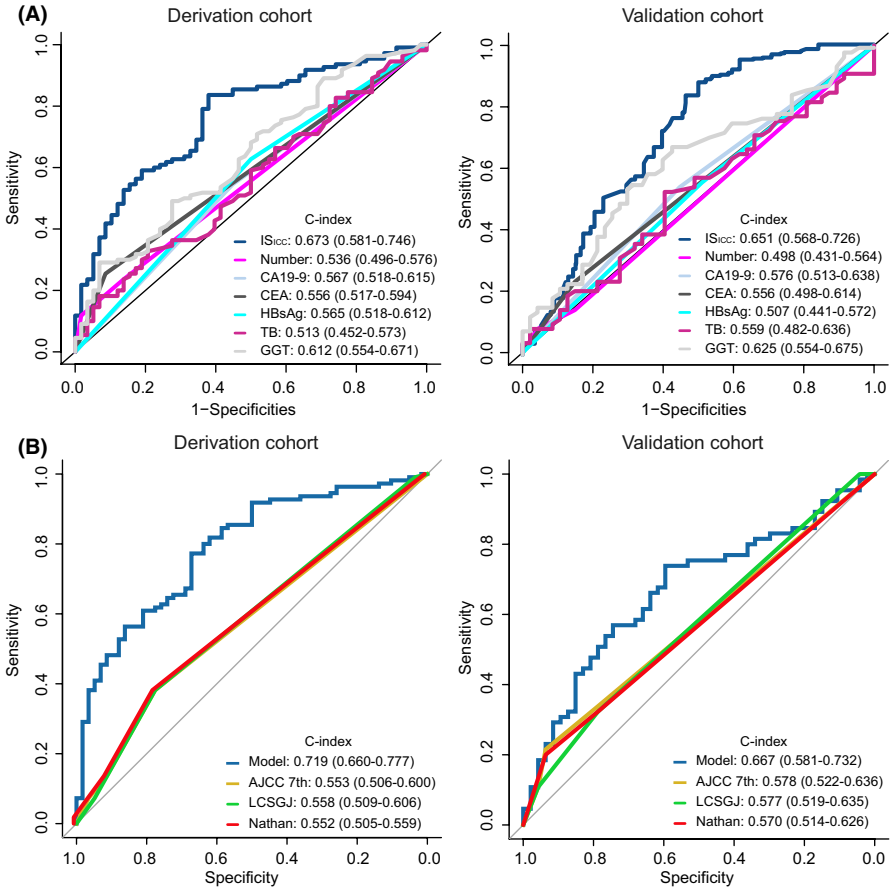

FIGURE 2 A, Receiver operating characteristic (ROC) curves for IS_{ICC} and six selected risk predictors in the derivation and validation cohorts. B, ROC curves for IS_{ICC}-applied prediction model and three traditional staging systems in the derivation cohort and the validation cohort

TABLE 3 Comparison of prognostic performance among 3 staging systems and the stratified IS_{ICC}-applied prediction model in the derivation cohort and validation cohort

Model	Derivation cohort		Validation cohort	
	Homogeneity (Wald χ^2)	AIC	Homogeneity (Wald χy^2)	AIC
Stratified IS_{ICC}-applied prediction model	39.3	1017.5	17.8	648.6
AJCC 7th for ICC	6.0	1050.8	9.4	657.0
Nathan	6.1	1052.7	7.1	659.3
LCSGJ	7.3	1049.5	7.5	658.9

Abbreviations: AIC, Akaike information criteria; AJCC, American Joint Committee on Cancer; IS_{ICC}, immune signature for ICC; LCSGJ, Liver Cancer Study Group of Japan.

various immune components in neoplastic or adjacent non–neoplastic specimens using the CIBERSORT method. Reductions of plasma cells, Tfh, macrophages and NK cells were observed in neoplastic tissues of the GSE76297 dataset. Consistent with the results for GSE76297 and HCC,[26] the intratumoral density of $CD68^+$, $CD57^+$, $CD27^+$ and $CD103^+$ cells was significantly lower than for the adjacent liver tissues, suggesting a generalized immunosuppressive status of ICC's intratumoral environment.

In the present study, four types of immune cells (CD3, CD45RA, CD57 and PD-L1) were identified in adjacent non–tumor tissues, and one (CD66b) in neoplastic tissues. Inconsistent with previous studies on ICC[27] or HCC,[28] we observed that the density of peritumoral $CD3^+$ cells was associated with patient survival. CD45RA (an immune marker of naïve T cells) exhibited reduced sensitivity to oxidative stress-induced cell death while maintaining their suppressive function.[29] Kenji et al reported that $CD8^+CD45RA^+CD62L^+CXCR3^+CD73^+$ young memory T cells were associated with drug resistance.[30] Growing evidence has revealed the negative correlation between high density of tumor-infiltrating NK cells (CD57) and metastasis in gastrointestinal sarcoma patients.[31] In our study, we found that peritumoral NK cells, rather than intratumoral NK cells, were associated with long-term survival, implying that the immune status of peritumoral tissues may also influence the evasion and metastasis of tumor cells. Expression of PD-L1 in tumor cells has been associated with improved response to anti–PD-1/PD-L1 inhibitors in patients with lung cancer.[32] Notably, peritumoral $PD\text{-}L1^+$ immune cells were also identified in our study. Intratumoral neutrophils (CD66b) have been revealed to be a poor prognostic factor for various types of cancers;[10,33] we observed similar results in ICC patients. Unlike inflammation-driven HCC, ICC is frequently accompanied by a dense desmoplastic stroma surrounding the malignant ducts and glands. The distinct carcinogenesis and biologic behaviors might be the reasons that 4 peritumoral immune features, out of 5 features, were correlated with patient survival in our study.

Of all tumor characteristics, tumor number was included in our final model. In accordance with previous study,[34] the presence

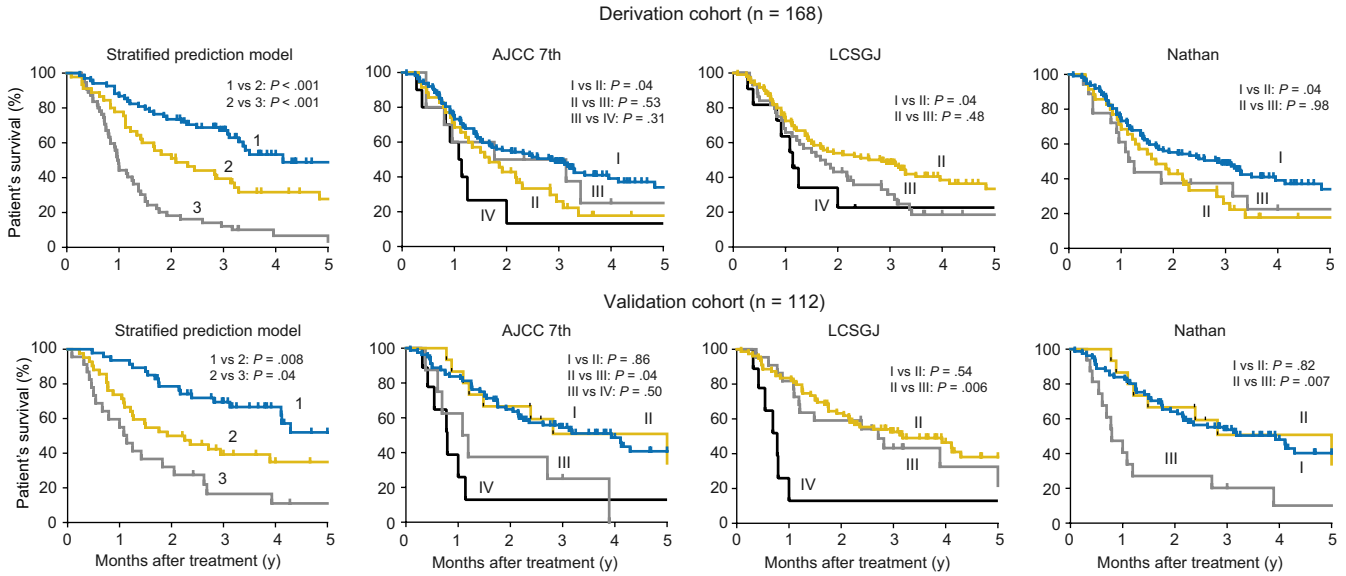

FIGURE 3 Kaplan-Meier survival curves of the derivation cohort and the validation cohort categorized by different staging systems (stratified prediction model; AJCC 7th for ICC; LCSGJ; Nathan)

of multiple nodules was an independent factor that affected patient survival. In our previous studies,[35,36] CA19-9 and CEA were identified as prognostic serum markers for liver cancer patients. Higher CA19-9[36] and CEA[34] levels were associated with advanced TNM stages and poor prognosis in ICC patients. The status of liver function also influences patient survival. In this study, GGT was identified as one of the prognostic predictors. The IS_{ICC}-applied prediction model based on these clinical and immunological predictors demonstrated better performance in terms of patients' survival prediction.

A few limitations should be noted in our study. First, the prognostic model was established based on data from one single liver center in China. Second, only patients with resectable ICC were enrolled in this study, and the HBV-related ICC accounted for 42.1% of the entire cohort. It remains to be explored whether our IS_{ICC}-applied prediction model is applicable to other patients. Third, further investigations are necessary to elucidate the underlying biologic mechanisms of the candidate markers, such as CD3, CD45RA, CD57, PD-L1 and CD66b.

In conclusion, our histological evidence-based prediction model was superior to current staging systems in predictive performance based on immune profile investigations and application of individualized immune signature. Further studies are needed to validate its predictive accuracy for prognosis and use for clinical application.

ACKNOWLEDGEMENTS

We express our sincere thanks to Jun Jiang and Wei Le for their contribution to bioinformatics, and Zunsong Hu and Wenjun He for statistical analysis. This work was supported by grants from the National High Technology Research and Development Program (863 Program) of China (2015AA020401), the National Natural Science Foundation of China (No. 81472674, 81530077, 81502486, 81773067, 81902963 and 81800790), and the Shanghai Committee of Science and Technology, China (No. 16JC1404000). The work was also sponsored by the Shanghai Sailing Program (19YF1407800 and 19YF1404300), the Shu Guang Project of the Shanghai Municipal Education Commission and Shanghai Education Development Foundation (13SG04), the Shanghai Municipal Science and Technology Major Project (Grant No. 2018SHZDZX05) and the China Postdoctoral Science Foundation (2018M640343 and 2019T120305).

CONFLICT OF INTEREST

The authors declare no conflict of interest.

ORCID

Mengxin Tian https://orcid.org/0000-0002-5315-1780
Shushu Song https://orcid.org/0000-0001-6261-8664
Yinghong Shi https://orcid.org/0000-0002-1833-8988

REFERENCES

1. Ercolani G, Vetrone G, Grazi GL, et al. Intrahepatic cholangiocarcinoma: primary liver resection and aggressive multimodal treatment of recurrence significantly prolong survival. *Ann Surg*. 2010;252:107-114.
2. Endo I, Gonen M, Yopp AC, et al. Intrahepatic cholangiocarcinoma: rising frequency, improved survival, and determinants of outcome after resection. *Ann Surg*. 2008;248:84-96.
3. Nepal C, O'Rourke CJ, Oliveira DV, et al. Genomic perturbations reveal distinct regulatory networks in intrahepatic cholangiocarcinoma. *Hepatology*. 2018;68:949-963.
4. Denkert C, von Minckwitz G, Darb-Esfahani S, et al. Tumour-infiltrating lymphocytes and prognosis in different subtypes of breast cancer: a pooled analysis of 3771 patients treated with neoadjuvant therapy. *Lancet Oncol*. 2018;19:40-50.
5. Jiang Y, Zhang Q, Hu Y, et al. ImmunoScore signature: a prognostic and predictive tool in gastric cancer. *Ann Surg*. 2018;267(3):504-513.
6. Wang JT, Li H, Zhang H, et al. Intratumoral IL17-producing cells infiltration correlate with antitumor immune contexture and improved response to adjuvant chemotherapy in gastric cancer. *Anna Oncol*. 2019;30:266-273.

7. Nywening TM, Belt BA, Cullinan DR, et al. Targeting both tumour-associated CXCR2(+) neutrophils and CCR2(+) macrophages disrupts myeloid recruitment and improves chemotherapeutic responses in pancreatic ductal adenocarcinoma. *Gut*. 2018;67:1112-1123.
8. Wang W, Green M, Choi JE, et al. CD8(+) T cells regulate tumour ferroptosis during cancer immunotherapy. *Nature*. 2019;569:270-274.
9. Pages F, Kirilovsky A, Mlecnik B, et al. In situ cytotoxic and memory T cells predict outcome in patients with early-stage colorectal cancer. *J Clin Oncol*. 2009;27:5944-5951.
10. Gu FM, Gao Q, Shi GM, et al. Intratumoral IL-17(+) cells and neutrophils show strong prognostic significance in intrahepatic cholangiocarcinoma. *Ann Surg Oncol*. 2012;19:2506-2514.
11. Omichi K, Cloyd JM, Yamashita S, et al. Neutrophil-to-lymphocyte ratio predicts prognosis after neoadjuvant chemotherapy and resection of intrahepatic cholangiocarcinoma. *Surgery*. 2017;162:752-765.
12. Liu CL, Fan ST, Lo CM, et al. Hepatic resection for combined hepatocellular and cholangiocarcinoma. *Arch Surg*. 2003;138:86-90.
13. Edmondson HA, Steiner PE. Primary carcinoma of the liver: a study of 100 cases among 48,900 necropsies. *Cancer*. 1954;7:462-503.
14. Gao Q, Qiu SJ, Fan J, et al. Intratumoral balance of regulatory and cytotoxic T cells is associated with prognosis of hepatocellular carcinoma after resection. *J Clin Oncol*. 2007;25:2586-2593.
15. Tian MX, Liu WR, Wang H, et al. Tissue-infiltrating lymphocytes signature predicts survival in patients with early/intermediate stage hepatocellular carcinoma. *BMC Med*. 2019;17:106.
16. Li S, Xu F, Li H, et al. S100A8(+) stroma cells predict a good prognosis and inhibit aggressiveness in colorectal carcinoma. *Oncoimmunology*. 2017;6:e1260213.
17. Zhang JX, Song W, Chen ZH, et al. Prognostic and predictive value of a microRNA signature in stage II colon cancer: a microRNA expression analysis. *Lancet Oncol*. 2013;14:1295-1306.
18. Harrell FE Jr, Lee KL, Mark DB. Multivariable prognostic models: issues in developing models, evaluating assumptions and adequacy, and measuring and reducing errors. *Stat Med*. 1996;15:361-387.
19. Frank E, Harrell J. Hmisc: harrell miscellaneous. R Package version 3.9-2. http://CRAN.Rproject.org/package=Hmisc
20. Camp RL, Dolled-Filhart M, Rimm DL. X-tile: a new bio-informatics tool for biomarker assessment and outcome-based cut-point optimization. *Clin Cancer Res*. 2004;10:7252-7259.
21. Liu PH, Hsu CY, Hsia CY, et al. Prognosis of hepatocellular carcinoma: assessment of eleven staging systems. *J Hepatol*. 2016;64:601-608.
22. Marrero JA, Fontana RJ, Barrat A, et al. Prognosis of hepatocellular carcinoma: comparison of 7 staging systems in an American cohort. *Hepatology*. 2005;41:707-716.
23. Chaisaingmongkol J, Budhu A, Dang H, et al. Common molecular subtypes among Asian hepatocellular carcinoma and cholangiocarcinoma. *Cancer Cell*. 2017;32:57-70.e3.
24. Garnelo M, Tan A, Her Z, et al. Interaction between tumour-infiltrating B cells and T cells controls the progression of hepatocellular carcinoma. *Gut*. 2017;66:342-351.
25. Gentles AJ, Newman AM, Liu CL, et al. The prognostic landscape of genes and infiltrating immune cells across human cancers. *Nat Med*. 2015;21:938-945.
26. Zhu XD, Zhang JB, Zhuang PY, et al. High expression of macrophage colony-stimulating factor in peritumoral liver tissue is associated with poor survival after curative resection of hepatocellular carcinoma. *J Clin Oncol*. 2008;26:2707-2716.
27. Noda T, Shimoda M, Ortiz V, Sirica AE, Wands JR. Immunization with aspartate-beta-hydroxylase-loaded dendritic cells produces antitumor effects in a rat model of intrahepatic cholangiocarcinoma. *Hepatology*. 2012;55:86-97.
28. Gabrielson A, Wu Y, Wang H, et al. Intratumoral CD3 and CD8 T-cell densities associated with relapse-free survival in HCC. *Cancer Immunol Res*. 2016;4:419-430.
29. Mougiakakos D, Johansson CC, Kiessling R. Naturally occurring regulatory T cells show reduced sensitivity toward oxidative stress-induced cell death. *Blood*. 2009;113:3542-3545.
30. Brunner SM, Itzel T, Rubner C, et al. Tumor-infiltrating B cells producing antitumor active immunoglobulins in resected HCC prolong patient survival. *Oncotarget*. 2017;8:71002-71011.
31. Delahaye NF, Rusakiewicz S, Martins I, et al. Alternatively spliced NKp30 isoforms affect the prognosis of gastrointestinal stromal tumors. *Nat Med*. 2011;17:700-707.
32. Ilie M, Szafer-Glusman E, Hofman V, et al. Detection of PD-L1 in circulating tumor cells and white blood cells from patients with advanced non–small-cell lung cancer. *Ann Oncol*. 2018;29:193-199.
33. Li YW, Qiu SJ, Fan J, et al. Intratumoral neutrophils: a poor prognostic factor for hepatocellular carcinoma following resection. *J Hepatol*. 2011;54:497-505.
34. Wang Y, Li J, Xia Y, et al. Prognostic nomogram for intrahepatic cholangiocarcinoma after partial hepatectomy. *J Clin Oncol*. 2013;31:1188-1195.
35. Shi RY, Yang XR, Shen QJ, et al. High expression of Dickkopf-related protein 1 is related to lymphatic metastasis and indicates poor prognosis in intrahepatic cholangiocarcinoma patients after surgery. *Cancer*. 2013;119:993-1003.
36. Jiang W, Zeng ZC, Tang ZY, et al. A prognostic scoring system based on clinical features of intrahepatic cholangiocarcinoma: the Fudan score. *Ann Oncol*. 2011;22:1644-1652.

SUPPORTING INFORMATION

Additional supporting information may be found online in the Supporting Information section.

How to cite this article: Tian M, Liu W, Tao C, et al. Prediction of overall survival in resectable intrahepatic cholangiocarcinoma: IS_{ICC}-applied prediction model. *Cancer Sci*. 2020;111:1084–1092. https://doi.org/10.1111/cas.14315